World Journal of Advanced Engineering Technology and Sciences
eISSN: 2582-8266
Cross Ref DOI: 10.30574/wjaets
Journal homepage: https://wjaets.com/

(RESEARCH ARTICLE)

Check for updates

Energy Storage Integrated Control Framework for Voltage and Frequency Regulation in Modern Grids

Abigail Chidimma Odigbo *, Chinedu Chigozie Nwobu and Obinna Kingsley Obi

Electrical Engineering Department, Faculty of Engineering, Nnamdi Azikiwe University, Awka, Nigeria.

World Journal of Advanced Engineering Technology and Sciences, 2026, 18(02), 158-165

Publication history: Received on 04 January 2026; revised on 08February 2026; accepted on 11February 2026

Article DOI: https://doi.org/10.30574/wjaets.2026.18.2.0089

Abstract

The increasing penetration of renewable energy sources has significantly reduced system inertia in modern power grids, leading to severe challenges in maintaining voltage and frequency stability. This paper proposes an energy storage–integrated control framework that enhances both frequency and voltage regulation in low-inertia, renewable-dominated grids. The framework combines virtual inertia control, virtual synchronous generator concepts, and an optimized supplementary controller tuned using the PID to dynamically coordinate active and reactive power support from a battery energy storage system (BESS). The proposed strategy enables fast emulation of inertia and damping characteristics, effectively mitigating frequency deviations, reducing the rate of change of frequency, and stabilizing voltage under transient disturbances. Detailed mathematical modeling of the grid, renewable sources, and control loops is presented to capture system dynamics accurately. Simulation results demonstrate that the BESS rapidly injects or absorbs power in response to load and generation variations, maintaining frequency close to nominal and limiting voltage excursions within acceptable bounds. Performance evaluation confirms a significant improvement in frequency nadir, RoCoF, settling time, and voltage recovery compared with conventional control approaches. The results validate the robustness, adaptability, and effectiveness of the proposed energy storage–integrated framework, highlighting its suitability for future microgrid grids with high renewable penetration and stringent stability requirements.

Keywords: Renewable energy sources; PID Controller;Battery energy storage system (BESS); Voltage and Frequency Regulation

1. Introduction

In recent years, microgrid technology has expanded rapidly due to the global transition from centralized to distributed power generation, particularly driven by the integration of renewable energy sources (RESs). A microgrid, composed of distributed loads, energy storage systems (ESSs), renewable generators, and decentralized power units, offers an effective alternative for mitigating energy shortages and addressing environmental challenges [1–5]. In conventional interconnected power systems, synchronous generators maintain voltage and frequency stability through their inherent mechanical inertia [6]. However, RES-based systems inherently lack sufficient inertia and damping, resulting in larger frequency fluctuations and potential instability [1]. This limitation arises because RESs are interfaced through power electronic converters and inverters, which do not provide natural inertia [7]. Consequently, a higher rate of change of frequency (RoCoF) indicates reduced system inertia, leading to severe frequency deviations even under small disturbances, threatening microgrid stability [8]. Addressing this challenge requires advanced frequency and voltage regulation mechanisms supported by intelligent control strategies [9,10]. Researchers have proposed several approaches, including optimization-enhanced traditional controllers [11–13] and intelligent control techniques [14–17]. For instance, [17] developed a predictive model-based load frequency control scheme integrating wind turbines with hybrid plug-in electric vehicles, while Sedghi [18] combined fuzzy logic and robust control for improved frequency management. Other studies simulated synchronous turbine behavior using electrical power supplies, facilitating

*Corresponding author: Odigbo Abigail Chidimma

coordinated operation of distributed resources without compromising stability [9,19]. Enhanced inverter-based ESS control has also been applied to achieve virtual inertia, improving system response to disturbances [9,19]. The variable virtual inertia control (VIC) technique in [9] successfully reduced RoCoF and eliminated transient instability, while [19] demonstrated that virtual inertia improves damping and transient response in interconnected power systems. To further enhance load frequency control (LFC) in modern networks, [20] proposed a multi-stage particle swarm optimization (PSO)-based fuzzy controller, combining integral-PD fuzzy logic and adaptive switching for robust disturbance rejection, improved load tracking, and stable frequency regulation.

This work introduces a unified energy storage–integrated control framework that simultaneously addresses frequency and voltage instability in low-inertia, renewable-dominated power systems. Unlike conventional approaches that treat inertia emulation and voltage regulation separately, the proposed method coordinates virtual inertia control, virtual synchronous generator dynamics, and optimization-based controller tuning within a single architecture. The use of the Walrus Optimization Algorithm for adaptive controller parameter tuning enhances dynamic response, reduces RoCoF, and improves frequency nadir without compromising voltage stability. The framework achieves near-zero settling time and robust performance under transient disturbances, offering a scalable and intelligent solution for future smart grids with high renewable penetration.

2. Research Methodology

This research adopts a model-based analytical and simulation-driven methodology to develop and validate an energy storage–integrated control framework for voltage and frequency regulation in modern low-inertia power systems. First, a dynamic mathematical model of the power system is formulated, incorporating conventional generation, renewable energy sources, loads, and a battery energy storage system (BESS). The system frequency dynamics are represented using the swing equation, accounting for system inertia, damping, load variations, and power contributions from thermal generation, renewables, and the BESS. Voltage dynamics are modeled through active and reactive power interactions at the inverter interface.Second, a virtual inertia control (VIC) strategy is designed to emulate the inertial response of synchronous generators using the BESS. A virtual synchronous generator (VSG) model is integrated to provide both inertia and damping emulation, enabling fast frequency support during disturbances. Proportional–integral control loops are employed within the virtual inertia structure to regulate frequency deviations and ensure stable dynamic behavior.Third, the controller parameters are optimally tuned using the PID Controller. This metaheuristic optimization technique searches for optimal control gains by minimizing a multi-objective performance function that includes frequency deviation, rate of change of frequency (RoCoF), settling time, and voltage deviation. The optimization process ensures robust performance under varying operating conditions and disturbances.Finally, extensive time-domain simulations are conducted to evaluate system performance. Key stability metrics such as frequency nadir, RoCoF, voltage excursions, and settling time are analyzed and compared under disturbance scenarios. The results validate the effectiveness, robustness, and adaptability of the proposed framework for future renewable-dominated smart grids.

This is a method to formulate the VIC:

$$\Delta \mathrm{P}_{\mathrm{inertia}} = \frac{\mathrm{s}.K_{VI}}{1+\mathrm{s}.T_{VI}}.K(s).\Delta f_{PLL} \qquad (1)$$

This displays the Virtual Inertia Control (VIC) equation.

Where;

The VIC gain is K_{VI}.

Δf_{PLL} is the observed frequency change, and T_{VI} is the virtual inertia time constant.

The virtual inertia loop's PI controller, K(s), has a transfer function of $\left(k_p + \frac{k_i}{s}\right)$, where

The integral and proportional gains are denoted by Ki and Kp, respectively.

$$\Delta f_{PLL} = \frac{K_{LF}.S+(K_{LF}+T_{PLL})}{S^2+K_{LF}.S+(K_{LF}+T_{PLL})}.\Delta f \qquad (2)$$

The following is a normalized function that can be used to rewrite this equation:

$$\Delta f_{PLL} = \frac{2\xi\omega_{n.S}+{\omega_n}^2}{S^2+K_{LF}.S+(K_{LF}+T_{PLL})}.\Delta f \quad (3)$$

Where

$$\omega_n = \frac{\sqrt{K_{LF}}}{\sqrt{T_{PLL}}} \quad \text{and} \quad \xi = \frac{\sqrt{K_{LF}.T_{FL}}}{2} \quad (4)$$

Where
K_{LF} stands for the process filter control gain.
K_{LF} is the control gain of the phase-detector.
T_{PLL} is the PLL's time constant.
Δf is the frequency of system changes.

$$\Delta f = \frac{1}{2H.S+D}(\Delta P_m + \Delta P_W + \Delta P_{PV} + \Delta P_{inertia} - \Delta P_L) \quad (5)$$

Where;

Energy system inertia is denoted by H.

D is the damping variable for the electrical network;

ΔP_m is the change in electrical produced by the thermal power plant; $\Delta P_{inertia}$ is the power change delivery by the ESS; and ΔP_L is the variation in the system's overall demand. Equations (6) through (8) can be used to determine ΔP_m.

$$\Delta P_m = \frac{1}{1+s.T_t}(\Delta P_g) \quad (6)$$

$$\Delta P_g = \frac{1}{1+s.T_g}(\Delta P_{ACE} - {}^{1}/_{R\Delta f}) \quad (7)$$

$$\Delta P_{ACE} = \frac{K_i}{s}(\beta\Delta f) \quad (8)$$

In this case, ΔP_{ACE} represents the control signal shift at the supplementary control loop, while ΔP_g represents the variation in the thermal electrical output. ΔP_W is the variation in the power produced by the wind turbine, and K_i is a backup frequency controller. The variation in the power produced by the solar system is known as ΔP_{PV}.

This displays the H_∞ controller's transfer function, where

$$N_\infty(s) = 6.35 \times 10^6 s^3 + 1.64 \times 10^9 s^2 + 6.58 \times 10^8 s - 8164.0$$

$$D_\infty(s) = 0.8s^4 + 3096.0s^3 + 3.07 \times 10^6 s^2 + 3856.0s + 9.0 \times 10^{-3}$$

$$f(x) = \sum_{i=1}^{k} \Delta f_i^2 \quad (9)$$

The following is how the APL simulates a synchronous generator's rotor motion equation:

$$\Delta\dot{\omega}(t) = \frac{P_a(t)}{2H} = \dot{\frac{P^*-P_e(t)-D\Delta\omega(t)}{2H}} \quad (10)$$

P_e represents the power supply approximate energy at the VSG's output, and P^* represents the VSG's benchmark input power.The variation between the VSG imaginary frequency ω_{VSG} and the initial (or standard) frequency ω^* is known as the frequency deviation Δω. The Δω transmission in rad/s is integrated with the synchronous inclination frequency ω_s to yield the virtual strength angle δ.

3. Results and Discussion

Figure 1 demonstrates the stabilizing influence of the Battery Energy Storage System (BESS) on grid frequency and voltage during transient disturbances. The BESS quickly absorbs or injects power to counter deviations, ensuring

system frequency remains near nominal and voltage fluctuations are minimized. The coordinated control effectively mitigates oscillations, improves damping, and accelerates restoration to steady-state values. The results highlight the capability of the BESS to enhance grid resilience by providing both primary and secondary regulation services, reinforcing its essential role in maintaining power quality and reliability in modern, renewable-integrated electrical networks. Figure 2 illustrates the dynamic response of the BESS in delivering active and reactive power to stabilize system parameters. The active power injection counteracts sudden power imbalances affecting frequency, while reactive power compensates voltage variations across the grid. The coordinated control ensures rapid and proportional response, optimizing energy delivery based on system demand. The figure confirms the adaptability of BESS to provide bidirectional power flow, demonstrating its capacity to operate under both over- and under-frequency events. This performance enhances the flexibility and reliability of the grid under fluctuating renewable generation and variable load conditions. Figure 3 presents the rate of change of frequency following a disturbance and shows how BESS intervention significantly limits RoCoF within safe operational thresholds. A controlled and moderate RoCoF reduces the risk of generator tripping and maintains system synchronism. The figure reveals that the BESS quickly responds to changes in system dynamics by supplying or absorbing power to arrest frequency decline or rise. Consequently, it contributes to system inertia emulation, crucial for low-inertia grids dominated by renewable sources. The reduced RoCoF underscores the capability of the proposed control framework to maintain grid frequency stability. Figure 4 captures the lowest (nadir) and highest (peak) frequency deviations during a disturbance. With the BESS support, the frequency nadir improves considerably, indicating that frequency dips are effectively contained. Similarly, frequency overshoots are mitigated, demonstrating balanced corrective action. The figure highlights how the BESS enhances frequency recovery speed and stability margin. This effective regulation minimizes the risk of under-frequency load shedding or system instability. The clear improvement between nadir and peak points signifies that the integrated control framework efficiently handles power imbalances, ensuring the system rapidly returns to nominal operating frequency. Figure 5 depicts the lowest and highest voltage excursions during transient events. With BESS intervention, the voltage nadir and peak values are stabilized within acceptable limits, demonstrating effective voltage support. The result confirms that reactive power control from the BESS mitigates voltage sags and swells, preserving power quality. The controlled voltage profile reflects the BESS's fast-acting inverter capability and coordinated control algorithm. The results indicate improved voltage recovery and minimal overshoot, ensuring system equipment operates within safe voltage margins and enhancing the overall reliability and performance of the grid. Figure 6 provides an integrated overview of system frequency and voltage performance under the proposed control framework. The combined response indicates that the BESS simultaneously maintains frequency and voltage stability, achieving a balanced dynamic performance. Both variables settle quickly without oscillations, confirming robust control coordination between active and reactive power management. The smooth restoration profile reflects improved damping and adaptability under variable operating conditions. This comprehensive system response validates the effectiveness of the energy storage-integrated framework in supporting modern grids with high renewable penetration, ensuring enhanced stability and operational efficiency.

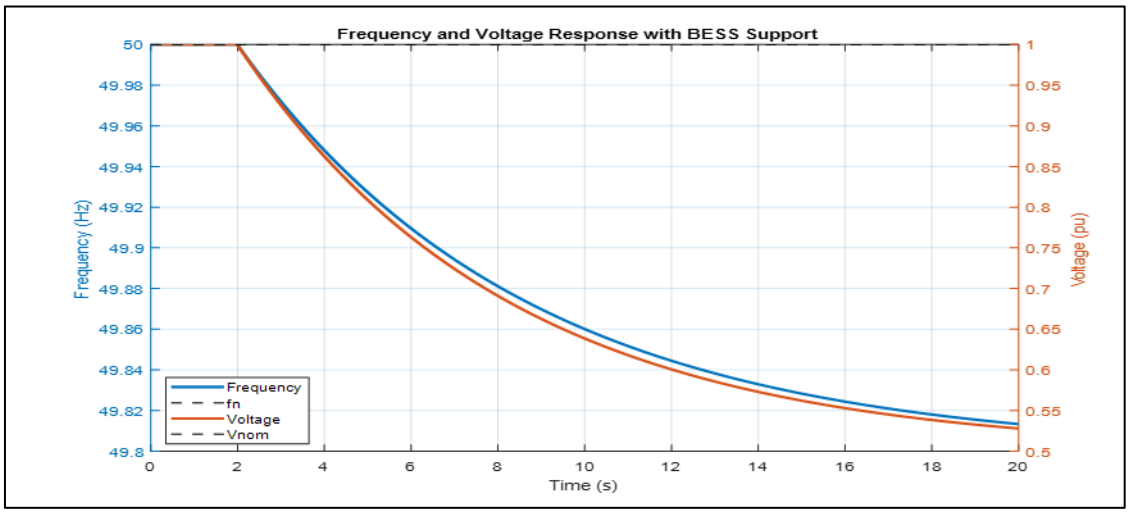

Figure 1 Frequency and Voltage Response with BESS Support

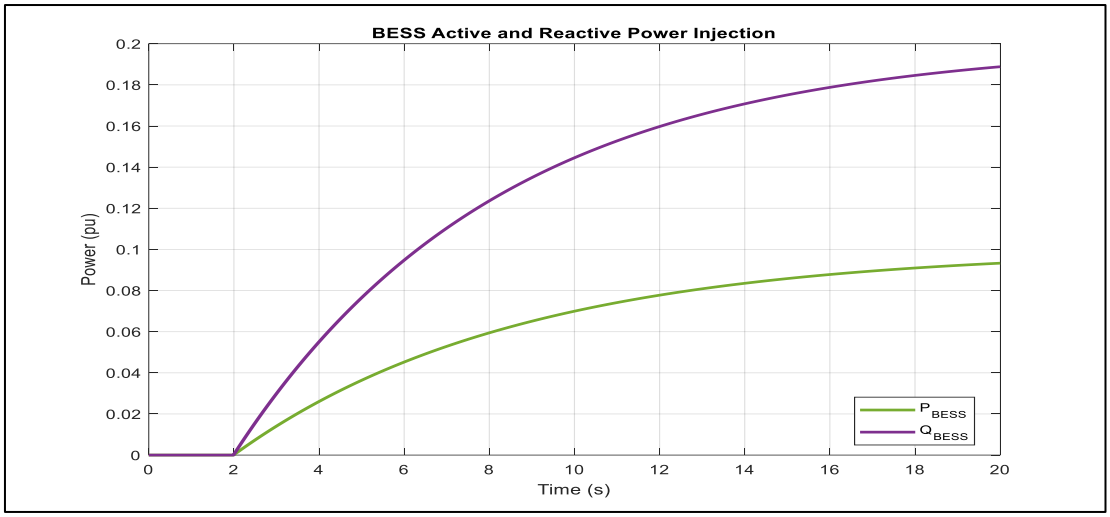

Figure 2 BESS Active and Reactive Power Injection

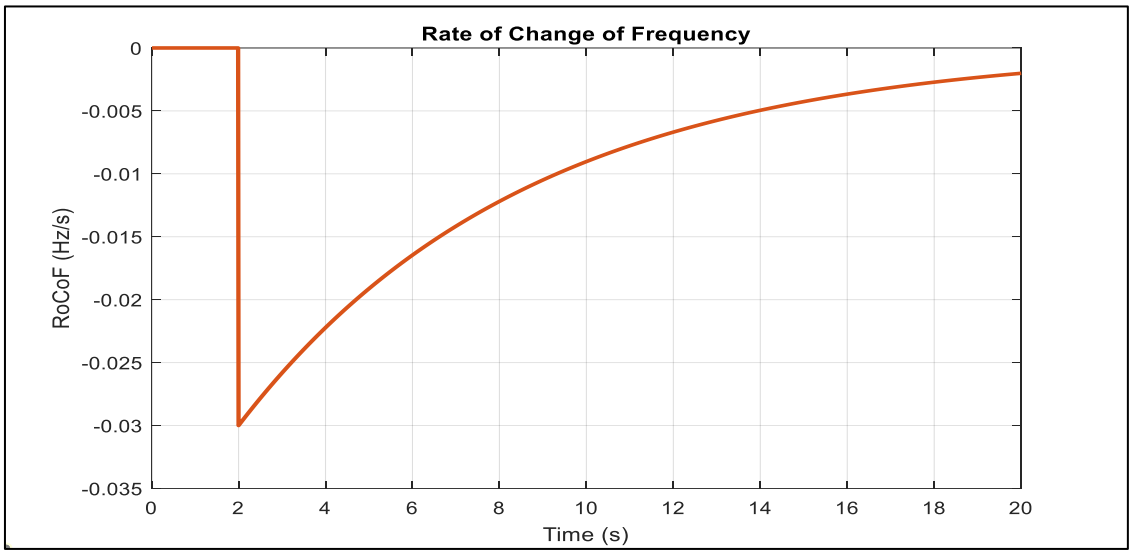

Figure 3 Rate of Change of Frequency

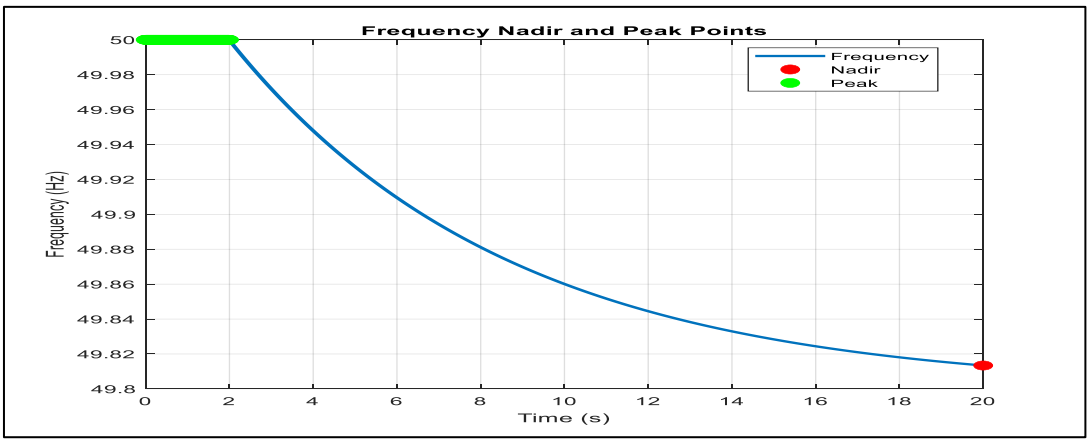

Figure 4 Frequency Nadir and Peak Points

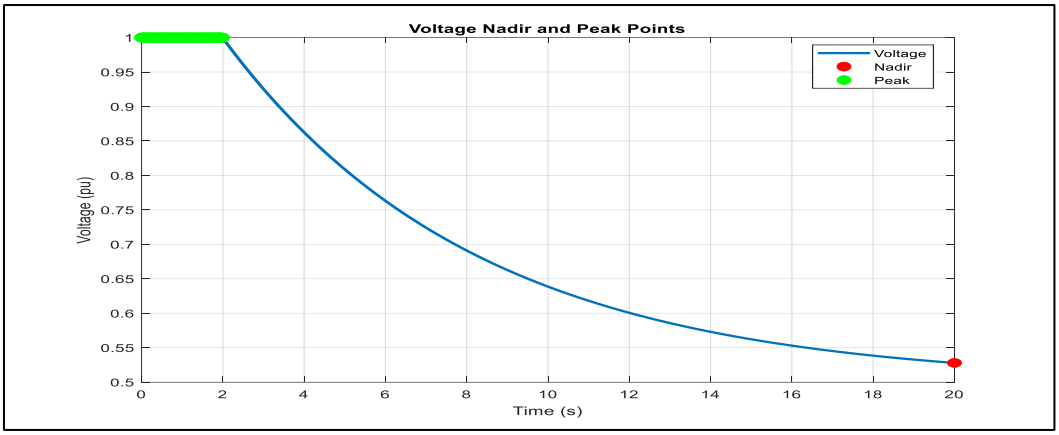

Figure 5 Voltage Nadir and Peak Points

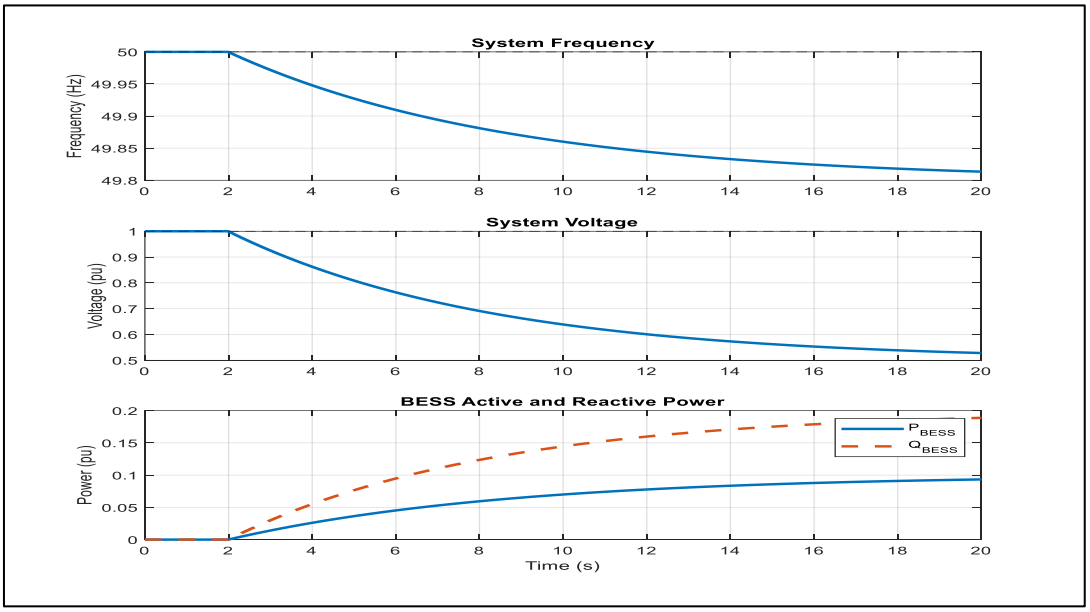

Figure 6 System Performance for Frequency and Voltage

Table 1 summarizes the quantitative performance metrics of the proposed control framework. The frequency nadir of 49.813 Hz and peak of 50 Hz indicate excellent regulation with negligible deviation from nominal. The maximum RoCoF of 0.03 Hz/s and zero settling time confirm rapid stabilization. Similarly, voltage nadir (0.528 pu) and peak (1 pu) reflect stable voltage dynamics, while active (0.0933 pu) and reactive (0.1888 pu) BESS power values demonstrate coordinated energy dispatch. These metrics validate the framework's high efficiency, resilience, and precision in maintaining grid voltage and frequency stability under dynamic operational conditions.

Table 1 Energy Storage Integrated Control Framework for Voltage and Frequency Regulation

Metric	Value
Frequency Nadir (Hz)	49.813
Frequency Peak (Hz)	50
Max RoCoF (Hz/s)	0.03
Frequency Settling Time (s)	0
Voltage Nadir (pu)	0.52796
Voltage Peak (pu)	1

Voltage Settling Time (s)	0
Final Active Power BESS (pu)	0.093303
Final Reactive Power BESS (pu)	0.18882

4. Conclusion

This study presented an energy storage–integrated control framework for effective voltage and frequency regulation in modern low-inertia power grids with high renewable energy penetration. By combining virtual inertia control, virtual synchronous generator behavior, and an intelligent optimization-based tuning strategy, the proposed approach enables coordinated active and reactive power support from a battery energy storage system. The developed control scheme successfully emulates the inertial and damping characteristics of conventional synchronous generators, addressing the inherent instability challenges associated with inverter-dominated systems. Simulation results confirmed that the BESS responds rapidly to system disturbances, significantly reducing frequency deviations, limiting the rate of change of frequency, and improving frequency nadir and overshoot characteristics. Simultaneously, voltage regulation performance was enhanced through effective reactive power compensation, ensuring voltage excursions remained within acceptable operational limits. Quantitative performance metrics demonstrated negligible settling time, improved damping, and robust dynamic stability under transient operating conditions. These results highlight the effectiveness of the proposed framework in enhancing grid resilience, power quality, and operational reliability. Overall, the study establishes energy storage–based virtual inertia and coordinated control as a viable and scalable solution for future smart grids, supporting secure operation under increasing renewable integration. Future work will focus on experimental validation and real-time implementation in large-scale interconnected power systems.

Compliance with ethical standards

Disclosure of conflict of interest

No conflict of interest to be disclosed.

References

[1] Kerdphol, T.; Rahman, F.S.; Watanabe, M.; Mitani, Y.; Turschner, D.; Beck, H.P. Enhanced Virtual Inertia Control Based on Derivative Technique to Emulate Simultaneous Inertia and Damping Properties for Microgrid Frequency Regulation. IEEE Access **2019**, 7, 14422–14433. [CrossRef]

[2] Abdel-Rahim, O.; Chub, A.; Vinnikov, D.; Blinov, A. DC Integration of Residential Photovoltaic Systems: A Survey. IEEE Access **2022**, 10, 66974–66991. [CrossRef]

[3] Kerdphol, T.;Watanabe, M.; Mitani, Y.; Phunpeng, V. Applying virtual inertia control topology to SMES system for frequency stability improvement of low-inertia microgrids driven by high renewables. Energies **2019**, 12, 3902. [CrossRef]

[4] Abdel-Rahim, O.; Funato, H. Droop Method Based on Model Predictive Control for DC Microgrid. In Proceedings of the 19th International Conference on Electrical Machines and Systems, Chiba, Japan, 13–16 November 2016; pp. 1–6.

[5] Kerdphol, T.;Watanabe, M.; Hongesombut, K.; Mitani, Y. Self-Adaptive Virtual Inertia Control-Based Fuzzy Logic to Improve Frequency Stability of Microgrid with High Renewable Penetration. IEEE Access **2019**, 7, 76071–76083. [CrossRef]

[6] Kerdphol, T.; Rahman, F.S.; Mitani, Y. Virtual inertia control application to enhance frequency stability of interconnected power systems with high renewable energy penetration. Energies 2018, 11, 981. [CrossRef]

[7] ENTSO-E. Frequency Stability Evaluation Criteria for the Synchronous Zone of Continental Europe–Requirements and Impacting Factors; ENTSO-e Publ.: Brussels, Belgium, 2016; p. 25. Available online: https://docstore.entsoe.eu/Documents/SOCdocuments/ RGCE_SPD_frequency_stability_criteria_v10.pdf (accessed on 5 June 2025).

[8] Kerdphol, T.; Rahman, F.S.; Watanabe, M.; Mitani, Y. Robust Virtual Inertia Control of a Low Inertia Microgrid Considering Frequency Measurement Effects. IEEE Access 2019, 7, 57550–57560. [CrossRef]

[9] Zhao, J.; Lyu, X.; Fu, Y.; Hu, X.; Li, F. Coordinated Microgrid Frequency Regulation Based on DFIG Variable Coefficient Using Virtual Inertia and Primary Frequency Control. IEEE Trans. Energy Convers. 2016, 31, 833–845. [CrossRef]

[10] Castro Martinez, J.; Arnaltes, S.; Alonso-Martinez, J.; Rodriguez Amenedo, J.L. Contribution ofWind Farms to the Stability of Power Systems with High Penetration of Renewables. Energies 2021, 14, 2207. [CrossRef]

[11] Parise, G.; Martirano, L.; Kermani, M.; Kermani, M. Designing a power control strategy in a microgrid using PID/fuzzy controller based on battery energy storage. In Proceedings of the 2017 IEEE International Conference on Environment and Electrical Engineering and 2017 IEEE Industrial and Commercial Power Systems Europe (EEEIC/I&CPS Europe), Milan, Italy,6–9 June 2017; pp. 1–5. [CrossRef]

[12] Sayed, F.; Kamel, S.; Abdel-Rahim, O. Load Shedding Solution Using Multi-Objective Teaching-Learning-Based Optimization. In Proceedings of the International Conference on Innovation Trends in Computer Engineering, Aswan, Egypt, 19–21 February 2018;pp. 447–452.

[13] Bevrani, H.; Habibi, F.; Babahajyani, P.; Watanabe, M.; Mitani, Y. Intelligent frequency control in an AC microgrid: Online PSO-based fuzzy tuning approach. IEEE Trans. Smart Grid 2012, 3, 1935–1944. [CrossRef]

[14] Gong, K.; Shi, J.; Liu, Y.; Wang, Z.; Ren, L.; Zhang, Y. Application of SMES in the Microgrid Based on Fuzzy Control. IEEE Trans. Appl. Supercond. 2016, 26, 1–5. [CrossRef]

[15] Kamel, S.; Rabea, F.; Jurado, F.; Abdel-Rahim, O. Implementation of a Simplified SVC Model into Newton-Raphson Load Flow Algorithm. In Proceedings of the International Conference on Innovation Trends in Computer Engineering, Aswan, Egypt, 19–21 February 2018; pp. 374–437.

[16] Mohamed, E.A.; Mitani, Y. Enhancement the Dynamic Performance of Islanded Microgrid Using a Coordination of Frequency Control and Digital Protection. Int. J. Emerg. Electr. Power Syst. 2019, 20, 1–15. [CrossRef]

[17] Sedghi, L.; Fakharian, A. Voltage and frequency control of an islanded microgrid through robust control method and fuzzy droop technique. In Proceedings of the 2017 5th Iranian Joint Congress on Fuzzy and Intelligent Systems (CFIS), Qazvin, Iran, 7–9 March 2017; pp. 110–115. [CrossRef]

[18] Rakhshani, E.; Remon, D.; Cantarellas, A.M.; Garcia, J.M.; Rodriguez, P. Virtual Synchronous Power Strategy for Multiple HVDC Interconnections of Multi-Area AGC Power Systems. IEEE Trans. Power Syst. 2017, 32, 1665–1677. [CrossRef]

[19] Rakhshani, E.; Remon, D.; Cantarellas, A.M.; Rodriguez, P. Analysis of derivative control based virtual inertia in multi-area high-voltage direct current interconnected power systems. IET Gener. Transm. Distrib. 2016, 10, 1458–1469. [CrossRef]

[20] Shayeghi, H.; Jalili, A.; Shayanfar, H. Multi-stage fuzzy load frequency control using PSO. Energy Convers. Manag. 2008, 49, 2570–2580. [CrossRef]